



## Spatio-temporal evolution and engineering implications of biofouling communities on floating wind turbines mooring lines

Antoine Dubois<sup>a,b,\*</sup>, Franck Schoefs<sup>a,b</sup>, Bruno Cognie<sup>a,b</sup>, Marine Reynaud<sup>c</sup>, Thomas Soulard<sup>c</sup>, Justine Dumay<sup>a,b</sup>

<sup>a</sup> ISOMer, UR2160, Nantes Université, 2 rue de la Houssinière, BP 92208, F-44000, Nantes, France

<sup>b</sup> Nantes Université, CNRS, IUML, FR CNRS 3473, F-44000, Nantes, France

<sup>c</sup> Fondation OPEN-C, 1 rue de la Noe, F-44321, Nantes, France

### ARTICLE INFO

#### Keywords:

Biofouling  
Marine growth  
Community dynamics  
Mooring lines  
Hydrodynamics  
Monitoring

### ABSTRACT

Mooring lines of floating offshore wind turbine (FOWT) provide a substrate for diverse biofouling species, thus ultimately influencing both ecological dynamics and their own structural performance. This study presents an analysis of spatial and temporal variations in community composition, coverage and thickness from the surface to the seabed through a four-year monitoring of biofouling development on two mooring lines of the FLOATGEN prototype. Along these lines, three distinct biofouling zones were identified with hard-bodied species dominating the water surface, mobile organisms prevalent at intermediate depths and soft-bodied species in deeper regions. Over time, biofouling coverage and thickness increased in deeper sections of the mooring lines, reflecting a progressive shift in community structure. A significant association was observed between fouling class (hard or soft), coverage and thickness, particularly in relation to depth. These results contribute to a better understanding of biofouling dynamics on floating offshore structures and underscore the need for reliable and standardized monitoring methods.

### 1. Introduction

Biocolonization communities (*i.e.* biofouling) play a key role in structuring marine ecosystems by impacting local biodiversity, trophic interactions and habitat availability (Markert et al., 2013; Rife, 2018; Sarà, 1986). The proliferation of man-made structures in the marine environment is increasing year on year, particularly as a result of offshore energy exploitation (Coolen et al., 2018; De Mesel et al., 2015; Vinagre et al., 2020), and these structures are undergoing this biocolonization. Since the 1990s, the offshore wind sector has experienced significant growth. Among the pioneering countries, Denmark, Germany, the Netherlands, the United Kingdom (Díaz and Guedes Soares, 2020) have turned their attention to such developments. It is also worth noting that these wind farms are being monitored, even though not in detail, not exclusively for scientific objectives but primarily to assess both the structural health condition and their effects on the maritime environment and ecosystems (Degraer et al., 2012, 2021). Any submerged structure at sea is bound to be promptly colonized by diverse organisms, and offshore renewable energy infrastructure is no exception

(Boukinda Mbadinga et al., 2007; Jusoh and Wolfram, 1996; Picken, 1984; Want et al., 2023). Among these, offshore wind turbines also serve as fully functional habitats as they can promote species recruitment, provide shelter and food (Causon and Gill, 2018; Raoux et al., 2018), and modify local hydrodynamics (Warby et al., 2024). However, physical and chemical parameters such as depth, substrate composition and hydrodynamic exposure can lead to distinct community assemblages (Vinagre et al., 2020).

Because of their inherent novelty and dynamic mooring systems, Floating Offshore Wind Turbines (FOWTs) pose distinct challenges for biofouling research and indicate that our understanding of the actual impacts of biocolonization on these types of structures is limited (Karlsson et al., 2022). The peculiar placement (*e.g.* vertical, sloping, or other) and constant movement in the water column of mooring lines can lead to intricate biofouling patterns, which may result in ecological niches that are distinct from those on stationary offshore infrastructures (Boukinda Mbadinga et al., 2007; Maduka et al., 2023; Pham et al., 2019a). Additionally, anthropogenic structures raise concerns regarding biological invasions (Elliott and Birchenough, 2022) and their impact on

\* Corresponding author. ISOMer, UR2160, Nantes Université, 2 rue de la Houssinière, BP 92208, F-44000, Nantes, France.

E-mail address: [antoine3.dubois@gmail.com](mailto:antoine3.dubois@gmail.com) (A. Dubois).

native biodiversity as they can act as a vector for non-indigenous species (NIS; De Mesel et al., 2015; Kerckhof et al., 2011; Mavraki et al., 2023) through the so-called stepping-stone effect (Bishop et al., 2017; Leclerc et al., 2019). Beyond these ecological considerations, biofouling introduces engineering challenges for developers of FOWTs as it can alter hydrodynamic loads (Decurey et al., 2020), increase the mass and drag forces, and create thermal insulation effects on submerged power cables (Maksassi et al., 2022, 2024). The accumulation of marine growth (*i.e.* biofouling) intrinsically modifies the roughness, the diameter and weight of FOWT's mooring lines (Marty et al., 2021, 2022), affecting their mechanical behavior and increasing maintenance costs (Ameryoun et al., 2019; Schoefs and Tran, 2022) and ultimately decreasing their service life. Biofouling can be categorized into several compartments comprising hard fouling organisms, including mussels, oysters, and tubeworms (Warby et al., 2024), or soft fouling organisms such as sea anemones, algae or soft corals (Coolen et al., 2018; De Mesel et al., 2015; Shi et al., 2012; Vinagre et al., 2020). These differences of classification can play a key role in drag forces exerted on the submerged components (Pham et al., 2019a). Indeed, soft fouling species are difficult to model, and therefore difficult to take into account in structural reliability assessment. Finally, soft fouling species have a different impact on component roughness, and therefore ultimately on hydrodynamic load, than hard fouling species (Decurey et al., 2020; Maduka et al., 2023).

Despite the growing number of operational floating wind farms, biofouling monitoring on FOWTs, and especially long-term studies, remains limited and restricts our understanding of their combined ecological and engineering implications. This study investigates the spatio-temporal evolution of biofouling communities on the mooring lines of FLOATGEN prototype, one of the world's first operational FOWTs deployed off the coast of Loire-Atlantique department in France

(Atlantic Ocean), to address this gap. It assesses species diversity, coverage of biofouling, and its thickness but also the potential impact of these parameters on the hydrodynamic loading of the mooring lines sampled. By examining two mooring lines with identical design, installation conditions and environmental exposure, the study aims to provide valuable and new insights into the biofouling processes on floating wind components and their broader implications for offshore wind farm monitoring and marine biodiversity.

## 2. Material & methods

### 2.1. FLOATGEN prototype and its mooring lines

The SEM-REV test-site, located 22 km off the coast of Le Croisic in the Atlantic Ocean at the South of Brittany in western France (Pays-de-la-Loire, France) with an area of 1 km<sup>2</sup>, was established from Ecole Centrale de Nantes and now administered by the OPEN-C Foundation (Fig. 1). The floating wind turbine sampled in this paper, FLOATGEN, is a semi-submersible concept equipped with Vestas V80 model with a capacity power of 2 MW. This FOWT was the inaugural French grid-connected offshore wind turbine, it was installed on-site on April 2018 and has been operated by BW IDEOL since that time. The square floater has dimensions of 36 m per side, a height of 9.5 m and a draft of 7.5 m, was constructed from reinforced concrete (patented Damping Pool® technology from BW IDEOL). The seakeeping is ensured by a semi-taut mooring system of six synthetic fiber (nylon) lines. The wind turbine is situated 12 nautical miles offshore at a water depth of 33 m (according to chart datum). The 50-year return value for the significant wave height is 9.6 m. The predominant and strongest current originates from the southwest tidal flow, with an average velocity (across the entire water

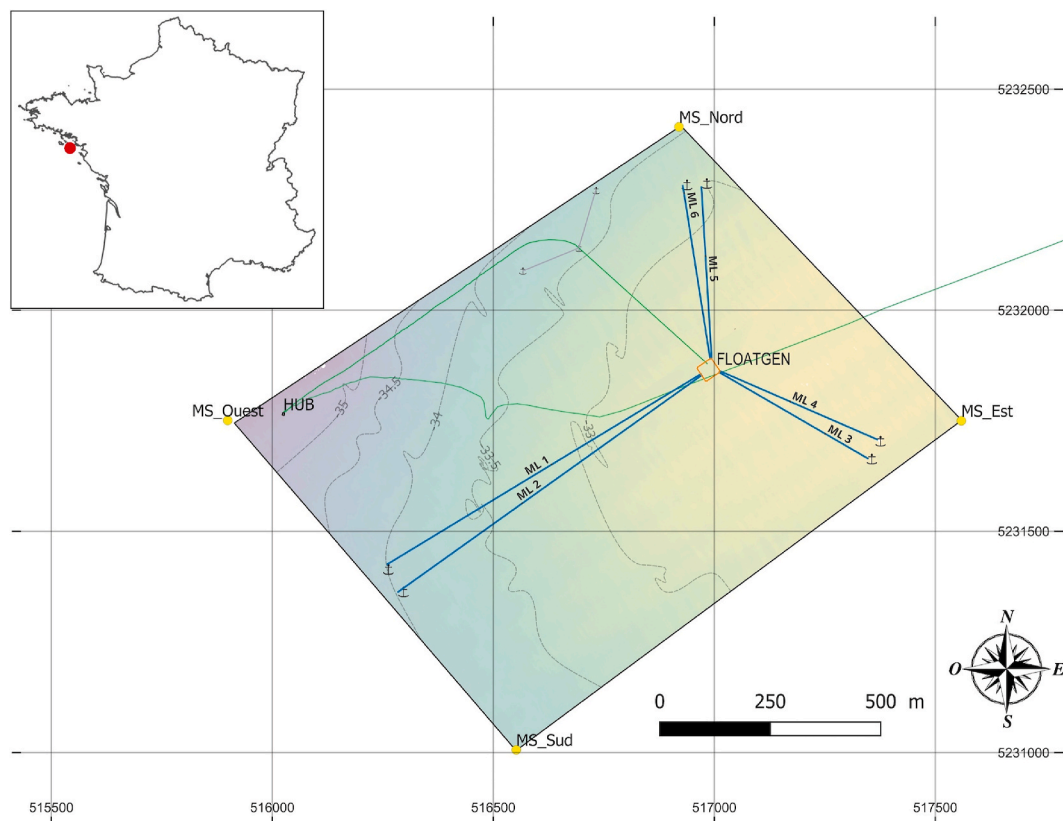


**Fig. 1.** Overview of the SEM-REV test site with the orientation of FLOATGEN's mooring lines (ML on the figure). Color gradients represent bathymetric levels (based on chart datum) with greater depth in blueish color and shallower depths for a yellowish color. The four buoys delimiting the site are represented with the MS acronym (Coordinate system EPSG: 32,630). (For interpretation of the references to color in this figure legend, the reader is referred to the Web version of this article.)

column) ranging from 0.2 to 0.4 m/s, while peak surface velocities reach up to 1.2 m/s and around 0.7 m/s a few meters above the seabed (Thilleul and Perignon, 2022).

During the summer of 2017, the mooring lines were installed on-site and wet stored a few meters above the seabed for nearly eight months (until April 2018), secured in place by anchors and floaters until the wind turbine was hooked up. FLOATGEN was integrated into the electrical grid in the end of 2018 summer.

## 2.2. Sampling method

The mooring lines have been regularly monitored since their installation using various Remotely Operated Underwater Vehicles (ROVs) and operators. The video recordings (samples) from these surveys, for two given mooring lines (ML4 and ML6 from Fig. 1), were used for the present study (Table 1). These lines were chosen because of their comparable exposure to currents and waves predominantly originating from the southwest. The similarities among these mooring lines maximized statistical robustness during testing. Additionally, one purpose was to examine whether there were key patterns of colonization along the lines, this information being crucial regarding predictability of bio-colonization's modeling in time and depth (e.g. in terms of colonization kinetics, community evolution, notable species and fouling classes).

Video recording (*i.e.* sampling) started near the water surface (3 m deep) and ended at a maximum depth of 34 m, depending on tide level. The recording was conducted in segments, comprising a total of 47 videos reviewed in their entirety all maintaining a resolution of 1024 by 576 pixels. The durations ranged from 56 s to 9 min and 40 s, resulting in nearly 2 h of video content analyzed. Video analysis was carried out as follows: the video was paused, selecting the best-quality frame at that depth. The same frame was used to estimate biocolonization coverage, followed by the calculation of its thickness. This was repeated at 1-m depth intervals. If the video frames were not of good quality (blurry, turbid, dark, ROV too far away) then an attempt was made to analyze them around 50 cm deeper. The mooring lines had diameters  $D$  of either 216 mm or 221 mm, respectively depending on the presence or absence of a special abrasion protection coating at particularly vulnerable sections of the mooring lines. This was indicated by a variation in color and texture of the line. Knowing the clean diameter  $x$  on the picture, the scale was obtained (Fig. 2).

This allowed the determination of biofouling thickness by calculating the difference between the actual diameter and the initial diameter using the standard equation:

$$th = \frac{1}{2} \left( \left( \frac{y \cdot D}{x} \right) - D \right) \quad (1)$$

where  $th$  stands for the thickness,  $D$  for the cylinder's (line) diameter,  $x$  the equivalent diameter on the picture, and  $y$  the colonized diameter (called effective diameter  $D_e$  in Maduka et al., 2023). The diameter of the colonized mooring line was measured at three distinct points,

**Table 1**  
Different ROVs and Vessels used for the mooring lines monitoring.

Year of Monitoring	ROVs Models	Recording features		Vessels
June 2019	BlueROV2	1080p (30 fps)	110° horizontal, 0.01 lux	JLD- MAELY
June 2020	ACHILLE	720p (30 fps)	2 * 250 W and 1 * 50 W halogen light	MINIBEX
June 2021	ARGOS ROV	1080p (30 fps)	4 * CTechnics Lights (4800 Lumen)	MINIBEX
June 2022	DEEP TREKKER REVOLUTION	1080p (30 fps)	0.001 lux, 260° Total range of view	ALKA BULLDOG

approximately 25–30 cm apart (see Fig. 2), on the same frame to get an average value for every meter of depth, thus minimizing the impact of outliers and measurement uncertainty as per Schoefs et al. (2009). ROVs were not equipped with a ruler comparable to Akxi3D® (Decurey et al., 2020; Schoefs et al., 2021) or with laser pointers to estimate lengths. As a consequence, the scale depicted in the image required a discernible section of uncolonized line. If the line was obscured or of poor quality (blurry, turbid, dark, ROV too far away), an attempt was made to measure 50 cm deeper; if the calculation remained unfeasible, a NA indicating uninterpretable data was entered for that frame. Consequently, the NA value can be explained by two primary factors:

- No reference on the image
- Poor image quality

This biofouling thickness computation yields a global thickness that encompasses the non-visible portion of the line, resulting in a uniform thickness around the entire line. The coverage is then computed based on the proportion of length (of the line) obscured by species, indicating that the original line is no longer visible. Biofouling coverage was visually estimated on a scale from 0 % to 100 %, with a 5 % increment. This factor has been shown to considerably influence the loading on cylinders (Schoefs et al., 2022; Zeinodini et al., 2017).

Finally, a taxonomic examination of the biofouling was conducted on the same frames as the thickness and coverage calculations. Taxonomy was performed to the lowest possible level (species, genus, order, class or phylum). The outcome was heavily contingent upon the quality of the ROV footage (with 2019–2020 being the lowest) and the proximity to the line. Consequently, if the analyzed image failed to facilitate taxonomic determination at any level, a NA was reported in the database for that image. NA denotes as follow:

- NA in thickness quantification
- NA in taxonomic determination

Each relative taxon abundance (presence) found on the frame was rated on a semi-quantitative scale ranging from 1 (few individuals) to 5 (many individuals). For data harmonization, all taxa were categorized based on the lowest identified common taxonomic level, which was the Family, or the Class for one specific taxon (*i.e.* Anthozoa). This identification facilitated the categorization of the taxa into a fouling class, which was classified as either soft (*e.g.* algae), hard (*e.g.* mussel) or mobile (*e.g.* sea urchin). Mobile fouling was analyzed separately from sessile biofouling. Finally, based on the reported quantities of each identified taxon in the image, the predominant (most prevalent of the image) fouling class was reported (*i.e.* hard, soft or mobile) for the image.

## 2.3. Data analysis

In the video analysis, the sample represented a single frame of the image, where all analyses were conducted. Based on the data on species occurrences beyond 16 m and the complexity of the collected data, depths were classified into three categories: 0–10 m, 11–15 m, and 16–33 m. Although the three categories showed varying amplitudes, this method allowed to gather a sufficient number of samples in each category, leading to acceptable confidence intervals when computing average values of thickness and coverage across multiple depths. These averages were then used to construct 95 % confidence intervals for each range.

The effect of the mooring line on biocolonization was assessed using an Unpaired Two-samples Wilcoxon test (Mann and Whitney, 1947; Wilcoxon, 1945) for each fouling category, as the data failed to meet the criteria for normal distribution as determined by the Shapiro test. Due to the complexity of the data, the impacts of depth and time were examined separately. A one-way ANOVA was conducted, contingent upon the

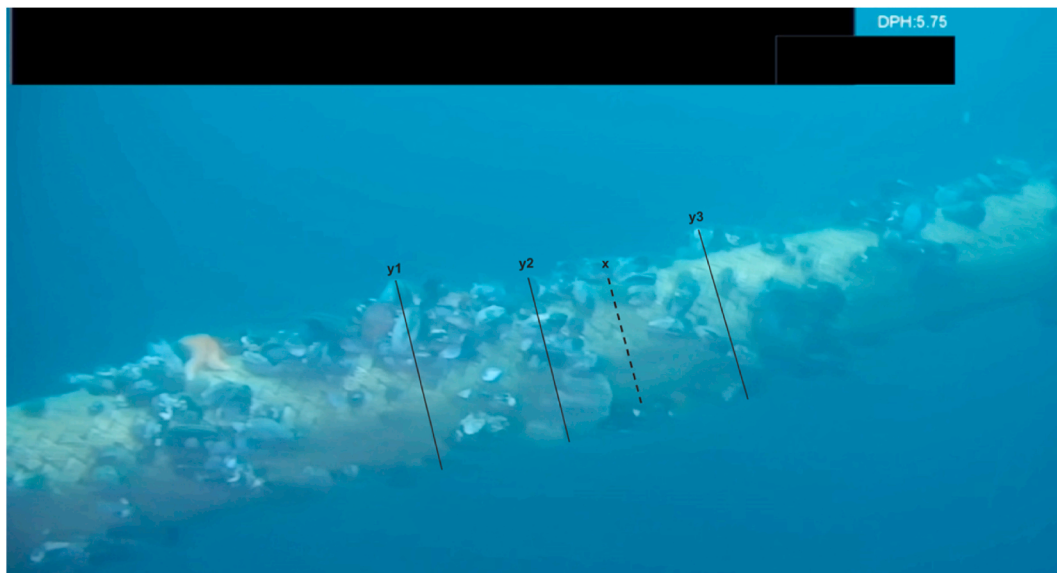


**Fig. 2.** Illustration of the lengths measured on one frame. Three positions (y1 to y3) were selected for equivalent diameter assessment to be compared with the reference diameter (x).

adherence to data normality and homogeneity, thereafter succeeded by a Tukey HSD test (Miller, 1981; Yandell, 1997). If not, a Kruskal-Wallis test was conducted, followed by a pairwise Wilcoxon rank sum test. All analyses were conducted utilizing R-studio (v2023.12.1 + 402) and R software (v4.3.1), incorporating the following packages: stats (v3.6.2), corrplot (v0.92), ggplot2 (v3.4.3), plyr (v1.8.8), and cowplot (v1.1.d). To visualize the depth distribution of each taxon, the kernel density estimation (KDE) was used with the `geom_density` function from the `ggplot2` package in R. This approach provides a smoothed representation of the relative frequency of taxon occurrences along the depth gradient. Note that in this context, ‘density’ refers to the probability density function of the depth distribution and not to the ecological concept of density (e.g. number of individuals per unit area). The models for evaluating the relationship between biofouling thickness and coverage were computed using the fundamental R software packages, particularly the ‘`lm ()`’ and ‘`subset ()`’ functions. The models analysis performed were replicated: measurements from the two lines for each year are compiled into a single database. The relationship between thickness and coverage was evaluated using both a linear, a quadratic (second-degree polynomial) and a logarithmic regression models for each fouling class. Model selection was based on adjusted  $R^2$  to assess explanatory power while accounting for complexity, and on p-values to ensure statistical significance. Residual diagnostics, including normality and homogeneity checks, were conducted to validate model assumptions. The final model for each fouling class was chosen based on the best balance between fit quality and statistical validity.

### 3. Results

#### 3.1. Biofouling diversity

A total of 170 frames were evaluated and extracted from recorded media (about 85 each line), with 48 not applicable (NA) reported for thickness evaluation and 16 NA for taxonomy determination, representing 28.2% and 9.4%, respectively. The aforementioned percentages are deemed acceptable, as these inspections are not designed for a quantitative evaluation of marine growth (Boukinda Mbadinga et al., 2007; Picken, 1984).

Eight classes were detected throughout the survey: Anthozoa, Asterozoa, Bivalvia, Cephalopoda, Echinozoa, Gastropoda, Ophiurozoa and Phaeophyceae. However, further identification was hindered

by video resolution, insufficient lighting or distance from the specimen for three of these classes: Anthozoa, Cephalopoda and Gastropoda. Eight distinct families were recorded as constituents of the biofouling community on the mooring lines: Alcyoniidae, Asterozoa, Corallimorphidae, Laminariaceae, Metridiidae, Mytilidae, Ophiotrichidae, and Parechinidae. Specimens were identified to the species level for eight taxa: *Alcyonium digitatum*, *Asterias rubens*, *Corynactis viridis*, *Laminaria digitata*, *Metridium senile*, *Mytilus edulis*, *Ophiotrix fragilis*, and *Psammechinus miliaris*. Few specimens of the Porifera phylum were recorded. No non-indigenous species (NIS) were recorded in the monitored duration of four years (monitored during early summer) and on two lines, but no physical sampling was carried out.

On the four years and two lines combined, the first 10 m were dominated by Mytilidae, with Laminariaceae being less prominent (Fig. 3). A transition occurred between 10 and 15 m in depth, characterized by the co-occurrence of Anthozoa-like organisms and member of the Anthozoa family: Metridiidae, alongside a few individuals of Mytilidae (Fig. 3). Fouling communities below 15 m were predominantly composed of *Metridium senile* (Metridiidae) and *Alcyonium digitatum* (Alcyoniidae; Fig. 3). Beyond 20 m, the community was dominated by Alcyoniidae. The gradient in community composition resulted in a notable transition (pairwise Wilcoxon test, p-value <0.001; Fig. 4) from predominantly hard fouling communities, which were solely located above 15 m depth, to a deep soft-fouling community found below this threshold. In addition, the transition zone was characterized by a significant presence of mobile fouling such as Asterozoa and Parechinidae (Fig. 4; Appendix 1). Furthermore, no significant difference (Wilcoxon tests, p-value >0.05; Fig. 4) between the two mooring lines examined was shown regarding fouling class assemblage, indicating that comparable exposure to current and wave conditions leads to similar distribution of species (section 2.2). In the first year of observation for both lines, all biofouling classes (i.e. soft, hard, mobile) were confined to near-surface depths, and by 2020, a trend of deeper colonization exclusively by soft fouling organisms (e.g. Metridii- and Alcyoniidae) emerged (Fig. 5). Conversely, hard fouling was always restricted to shallow parts of the mooring lines (close to the water surface). Mobile fouling taxa, including Asterozoa and Parechinidae, were recorded at depths ranging from 3 to 24 m, with their distribution confined to shallow waters, particularly in 2020 (Fig. 5). Predation events of *Asterias rubens* on *Mytilus edulis* were also recorded multiple times during video footage analysis, particularly in the first two years of monitoring

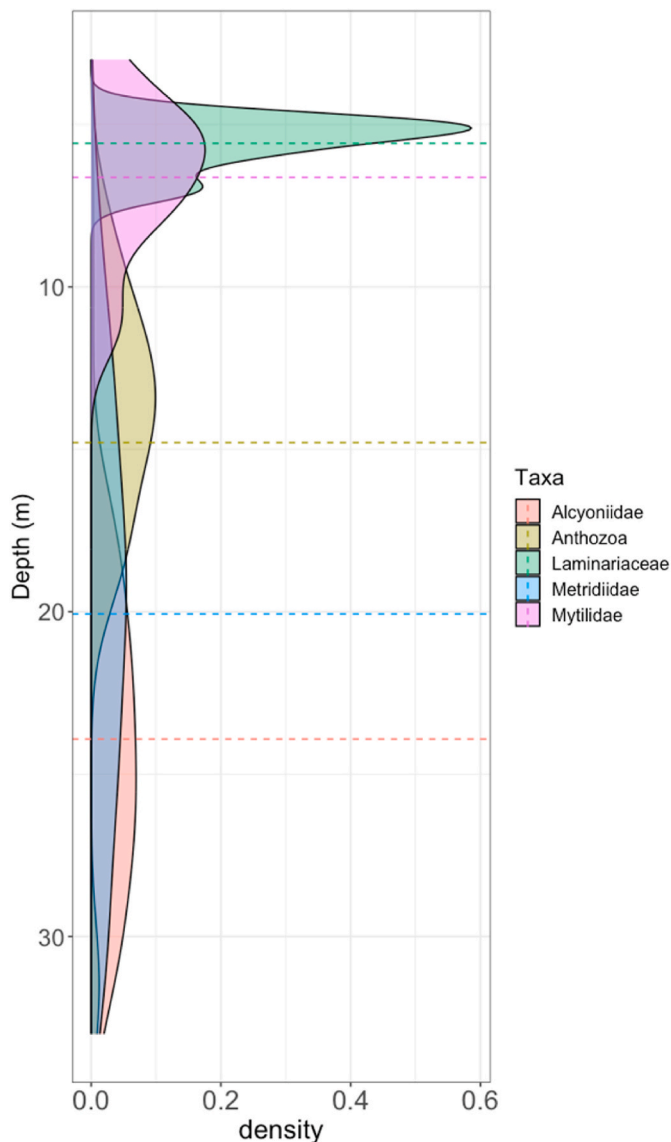


**Fig. 3.** Sessile taxa distribution along the depth profile - All year & line combined. Caption: Dashed lines represent the mean depth for each taxa. Anthozoa: 14.8 m, Mytilidae: 6.6 m, Metridiidae: 20.1 m, Alcyoniidae: 23.9 m, Laminariaceae: 5.6 m. Kernel density estimation (KDE) was used to represent the relative frequency of occurrences along the depth gradient. Density values correspond to the probability density of taxon occurrence, not individual abundance.

(Appendix 2).

### 3.2. Depth and time impacts on coverage

The statistical analysis of biofouling coverage highlights a depth-dependent pattern with significantly higher values recorded at [16–33] meters in 2022 with 95 % in average covered by biofouling compared to an average 62.5 % at [11–15] meters and 40.9 % at [0–10] meters depth (Fig. 6A). In deeper sections of the mooring lines ([16–33] meters), the coverage exceeds 80 % after one year, while in contrast, the other monitored years exhibit substantial variability (95 % confidence intervals), leading to non-significant differences across time (Fig. 6B). The temporal analysis further reveals that biofouling coverage at [0–10] meters was significantly greater in 2020 with 80.2 % covered in average compared to 2022 (Fig. 6B). However, at intermediate depths ([11–15] meters), coverage fluctuated over the four-year monitoring period, preventing the identification of clear statistical trends. Although

variations appear visually distinct at [16–33] meters, statistical tests were unable to prove a clear trend.

### 3.3. Spatio-temporal evolution of thickness

Biofouling thickness displayed marked spatial and temporal fluctuations (Fig. 7A and B). The highest thickness was recorded at [0–10] meters in 2020 (third year post-immersion) with 69.51 mm in average, whereas at [16–33] meters, maximum values occurred in 2022 (fifth year post-immersion) with a peak at 46.72 mm in average. Over time, thickness at greater depths increased significantly from the fourth year (*i.e.* 2021; Fig. 7B). A trend suggesting an increase at [0–10] meters was observed, yet statistical validation was lacking. The accumulation of biofouling resulted in thickness increases of the mooring lines ranging from +7 % ([11–15] meters in 2020) to +32 % ([0–10] meters in 2020), with an overall increase of +16 %. These variations have direct implications for structural loading, particularly in shallower sections where biofouling-induced mass gain is more pronounced.

### 3.4. Coverage - thickness relationship depending on fouling class

The kernel density estimation analysis reveals a clear distinction between mobile fouling and the classes of hard or soft fouling classes regarding their coverage (Fig. 8, upper density plot). The mobile fouling class predominantly exhibits coverage on mooring lines ranging from 0 to 60 %. Conversely, soft and hard fouling predominantly exhibit higher coverage percentages, typically ranging from 50 % to 100 %, while hard fouling exhibits a more consistent distribution, ranging from approximately 5 to 100 %, compared to soft fouling. The mean thickness of the mooring line indicates that each fouling class shows a peak representation within the range of 0–50 mm (Fig. 8, right density plot). Nonetheless, the hard fouling class exhibits a more consistent distribution for the thickness parameter and is the sole category to attain remarkable values exceeding 75 mm. With regard to soft fouling, this class was mostly distributed between 25 and 75 mm thickness, with a corresponding coverage of between 75 and 100 %.

The scatter diagram (Fig. 8, center plot) reveals a significant overall relationship between thickness and coverage. The analysis indicates a statistically significant linear regression model ( $p < 0.001$ ), accompanied by a low  $r^2$  ( $r^2 = 0.26$ ). Upon analysis of the three fouling classes, it is observed that the optimal fitting model ( $r^2 = 0.724$ ,  $p$ -value  $< 0.001$ ) for the hard fouling data is represented by a non-linear quadratic model of the following form:

$$\text{Thickness} = 0.027 * \text{Coverage}^2 - 2.181 * \text{Coverage} + 54.295 \quad (2)$$

Another non-linear model is found to better fit the mobile fouling class ( $r^2 = 0.31$ ,  $p$ -value  $< 0.01$ ) with the form of an affine function:

$$\text{Thickness} = 0.19 * \text{Coverage} + 13.277 \quad (3)$$

## 4. Discussion

### 4.1. Distribution of biofouling community across space and time

#### 4.1.1. Zonation and competition

Our investigation revealed a hard-fouling community in the uppermost layers of the water column, transitioning to soft organisms at greater depths (*i.e.* beyond 15 m), a typical stratification as described by Picken (1984) or Boukinda Mbadanga et al. (2007). A community dominated by Bivalvia (Mytilidae) and their predators (Asteroidea) was observed from the water surface to 10 m, followed by a transitional assemblage from 11 to 15 m (Appendix 3). Soft fouling organisms such as *Metridium senile* (Metridiidae) and *Alcyonium digitatum* (Alcyoniidae) became dominant below 15 m depth (Fig. 3). Colonization patterns evolved over time, with an initial settlement in shallower sections of mooring lines progressively extending to deeper sections. These

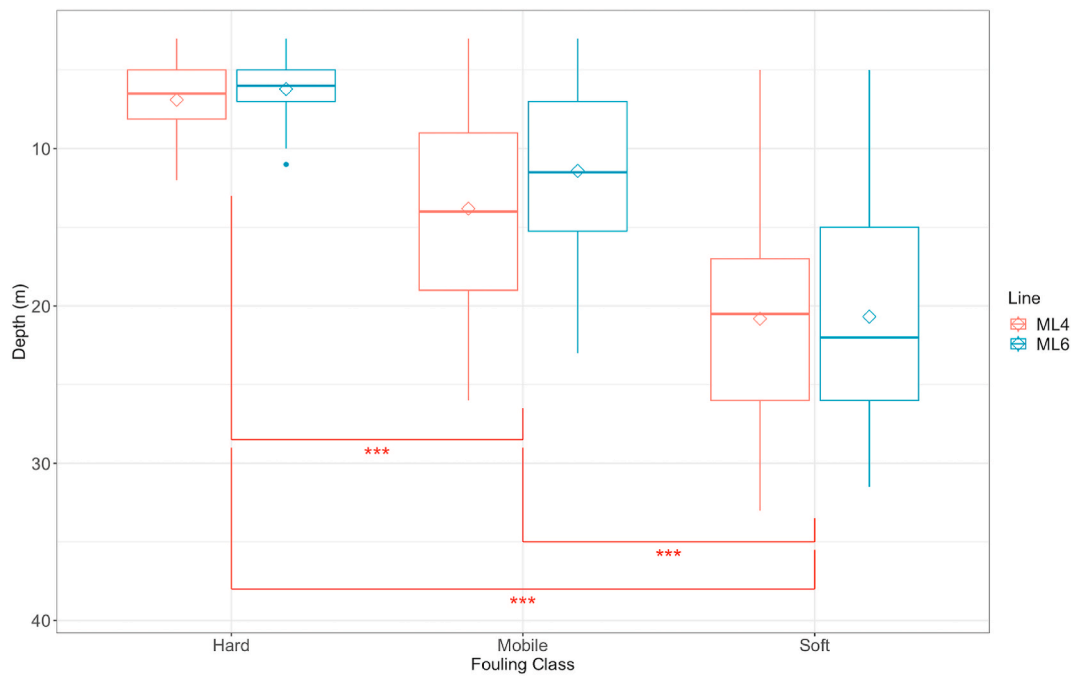


**Fig. 4.** Difference of depth occurrence for each fouling class depending on the mooring line surveyed, all years combined. Caption: no significant difference is found between mooring lines (Wilcoxon tests, p-value >0.05), black brackets indicate a significant difference between fouling classes all year and lines combined (pairwise Wilcoxon test, \*\*\*: p-value <0.001); squares indicate the mean depth for each class.

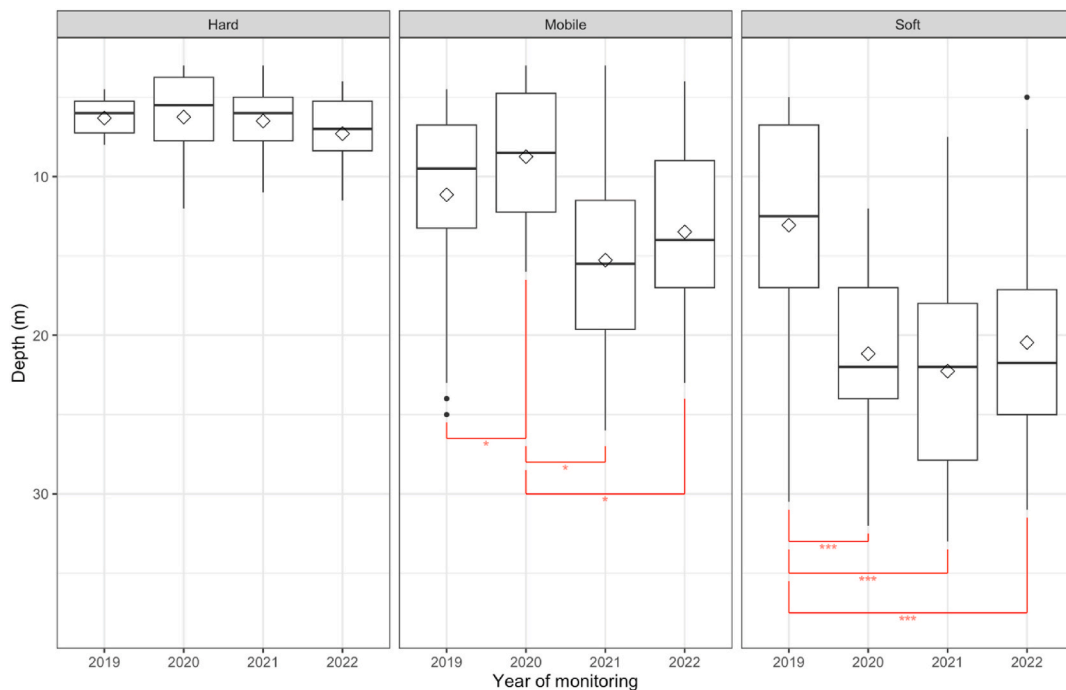


**Fig. 5.** Difference of depth range for each class of fouling depending on the monitored year, both lines combined. Caption: red brackets indicate a significant difference between year, pairwise Wilcoxon tests (\*: p-value <0.05 and \*\*\*: p-value <0.001). (For interpretation of the references to color in this figure legend, the reader is referred to the Web version of this article.)

dynamics reflect the depth preferences of each species and their ecological interactions. *Mytilus edulis* exhibits a marked preference for the intertidal zone where higher nutrient inputs are available (e.g. phytoplankton) and lower competition creates favorable conditions (Seed and Suchanek, 1992; Tyler-Walters, 2008). In contrast, *M. senile* and *A. digitatum* favor deeper hard substrates, a trend supported by observations on artificial structures at depths of 25–35 m (Torquato

et al., 2021; Want et al., 2023). Similar zonation patterns across depths were also documented on fixed offshore wind farms (e.g. De Mesel et al., 2015; Coolen et al., 2018).

The distribution of fouling classes (Fig. 8) indicated that soft organisms covered a greater area compared to hard or mobile species. This phenomenon may be explained by the reproductive strategies of these species (i.e. *M. senile* and *A. digitatum*). *M. senile* demonstrates asexual

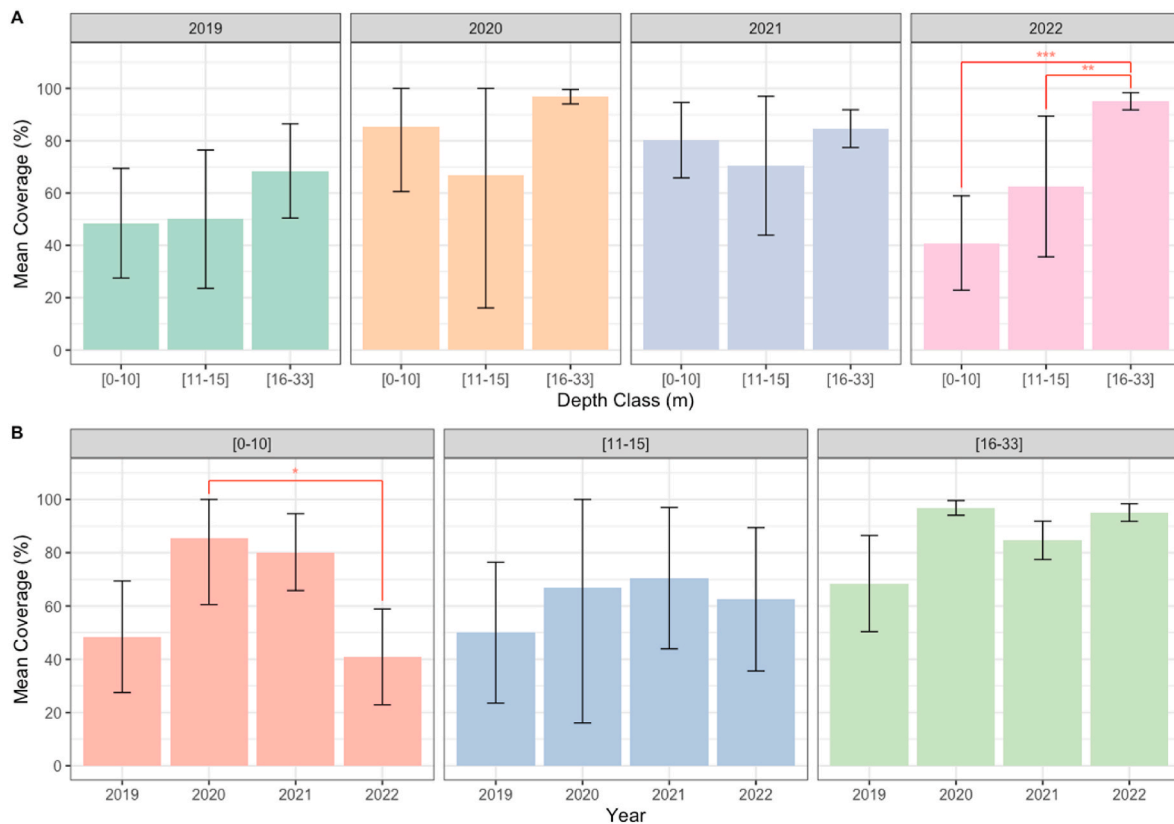


**Fig. 6.** A. Depth-driven variability in biofouling coverage (in %) across years. Caption: error bars represent Interval Confidence at 95 % threshold; Red brackets indicate a significant difference between two depth ranges Pairwise Wilcoxon test (\*\*: p-value <0.01 and \*\*\*: p-value <0.001). B. Temporal evolution of biofouling coverage (in %) at the different depth class. Caption: error bars represent Interval Confidence at 95 % threshold; Red bracket indicates a significant difference (One-way ANOVA, \*: p-value <0.05). (For interpretation of the references to color in this figure legend, the reader is referred to the Web version of this article.)

reproduction (cloning) for rapid habitat colonization and sexual reproduction for enhanced genetic diversity, facilitating effective colonization (Hiscock and Wilson, 2007). These organisms have the ability to move by sliding and cover other organisms (Nelson and Craig, 2011), as is frequently observed in mussel colonies. They can use their cnidocytes to sting adjacent organisms as a competitive strategy for spatial acquisition (Hiscock and Wilson, 2007). Numerous studies have shown that *M. senile* can significantly diminish species richness (Coolen et al., 2015, 2018; van der Stap et al., 2016; Whomersley and Picken, 2003) supporting its strong competitive advantage. Finally, all video recordings were unable to reveal the presence of natural predators of this anemone, such as *Spondyliosoma cantharus*. The species' dominance and apparent lack of predation could explain its proliferation over the years on the mooring lines. A similar lack of predation was also noted for *Alcyonium digitatum* as none of its predators were documented: small mollusks that inhabit areas linked with *A. digitatum* such as *Simnia patula* and *Tritonia hombergi* (Budd, 2008). Conversely, a high abundance of mobile predators, including *Asterias rubens* and *Psammechinus miliaris*, was documented during the first years of monitoring featuring multiple predation events of *A. rubens* on *Mytilus edulis*. A marked decline in predation was recorded post-2020 alongside a diminished presence of *M. edulis*, potentially due to increased predatory pressure. It is well acknowledged that predation is a key driver in structuring communities (De Mesel et al., 2015; Osman, 1977). The grazing behavior of *P. miliaris* may have significantly influenced species dominance on the mooring line by selectively feeding on small, solitary individuals, hence creating opportunities for fast-reproductive and rapidly growing species such as *M. senile* or *A. digitatum*.

Another plausible factor influencing fouling community distribution is the disturbance of the mooring lines, influenced by the localized impacts of waves and currents on the organisms, as recognized by both

industry and scientific fields (Almeida and Coolen, 2020; van der Stap et al., 2016). Indeed, the combination of motions of submarine assets and the waves and currents on fluid velocity can result in high local relative fluid velocities that may affect biofouling. The composition of mooring lines itself can also influence biocolonization in the context of "cleaning". Indeed, nylon can undergo several types of deformation, either longitudinally or radially (torsion). This can affect the mechanical tension and micro-spaces between the nylon fibers, changing the substrate properties for organism attachment.

#### 4.1.2. Succession and evolution

All evidence found in our study in the Atlantic Ocean suggests a community succession pattern comparable to that observed in the North Sea on artificial substrates (Degraer et al., 2012; Karlsson et al., 2022; Kerckhof et al., 2019) expected to evolve to a low-species-richness biotope (Connor et al., 2004) dominated by *M. senile* to potentially reach the EUNIS MC1-2281 habitat (PatriNat, 2023), or also JD-1.1 habitat (Lutrand et al., 2020). Nonetheless, it is crucial to compare these findings with long-term studies, such as those conducted at the Belgian Offshore Wind Farm. The first monopiles were installed in 2009, displayed a variable community composition within the first five years after immersion followed by a semblance of stable community; yet, after 11 years of immersion and monitoring, no definitive stable state (*i.e.* climax) was found (Zupan et al., 2023). Annual, seasonal, and sporadic events continuously alter the community, complicating predictions; even 11-year or 18-year monitoring periods may be inadequate or insufficient to reveal a temporal pattern on offshore structures such as oil platform (Almeida and Coolen, 2020; Whomersley and Picken, 2003). Concluding on a stable community is further complicated for example by the fact that Oshurkov (1992) demonstrated decades ago that mussel communities frequently exhibit cyclical dynamics lasting

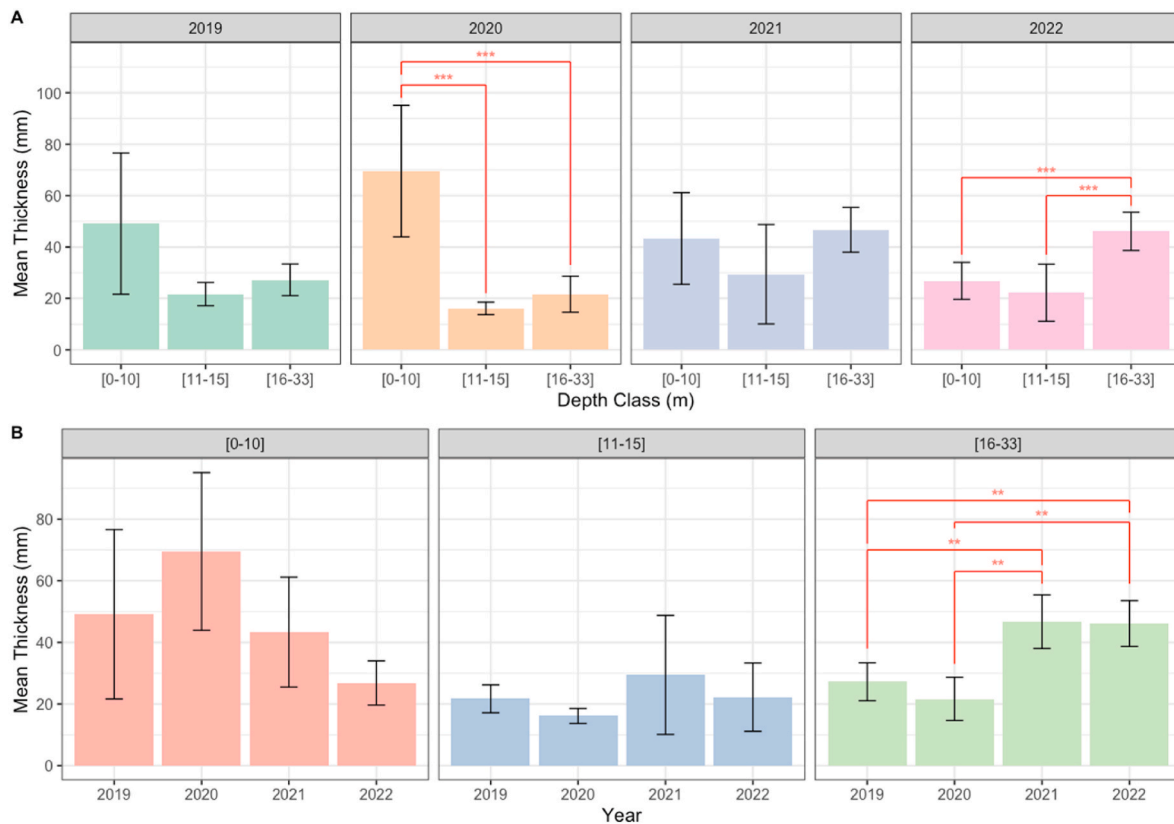


**Fig. 7.** A. Depth-driven variability in biofouling thickness (in mm) across years of monitoring. Caption: One-way ANOVA, p-value <0.001 (\*\*\*); error bars represent Interval Confidence at 95 % threshold; Red lines indicate a significant difference between two depth ranges. B. Temporal evolution of biofouling thickness (in mm) at the different depth class. Caption: error bars represent Interval Confidence at 95 % threshold; Red brackets indicate a significant difference between two years, Pairwise Wilcoxon test (\*\*: p-value <0.01). (For interpretation of the references to color in this figure legend, the reader is referred to the Web version of this article.)

around 10–20 years, rather than representing a permanent climax state. Our observations, along with previous studies (Coolen et al., 2018; Whomersley and Picken, 2003), suggest that in the absence of strong predation or competition, a relatively persistent assemblage dominated by *Metridium senile* and *Alcyonium digitatum* may establish over time (Appendix 4), while a fully stable climax community is unlikely (Zupan et al., 2023). The dominance of suspension feeders is consistent with long-term trends observed in other biofouling communities. Offshore oil rigs in the North Sea displayed a similar assemblage even after 40 years post-installation (Van Der Stap et al., 2016). Soft fouling species typically prevail in moderate current speeds (0.5 m/s) due to their relatively long body, which are susceptible to be damaged by higher current speeds (Budd, 2008; Hiscock and Wilson, 2007; Koehl, 1977). This could explain their low presence in the first 15 m of the water column (Fig. 4) where higher velocities are typically found. The vertical distribution of *Mytilus edulis* observed in this study, primarily restricted to the upper 10 m, may be partially explained by hydrodynamic exposure near the surface. *M. edulis* is known to dominate wave-exposed intertidal zones due to its strong attachment via byssal threads and dense patch communities, which are actively produced in response to wave action (Carrington, 2002). This morphological and behavioral adaptation likely provides a competitive advantage over soft-bodied species such as *M. senile* and *A. digitatum* in high-energy environments. Conversely, in deeper, more hydrodynamically stable conditions, soft-bodied species may be better suited to persist and outcompete bivalves. The dominant species found in our study were generally of significant stature and larger body size in comparison to other prevalent biofouling species such as tubeworms, barnacles or oysters (e.g. Want et al., 2023). This has broader ecological implications, as when scaled to an entire wind farm, these colonized substrates can significantly impact the pre-existing ecosystem. This was already observed in various offshore wind farms

(Causon and Gill, 2018; Kerckhof et al., 2019; Spielmann et al., 2023; Zupan et al., 2023) and work began to take the entire ecosystem into account in modeling (Maar et al., 2009; Niquil et al., 2020; Pezy et al., 2020). Indeed, the introduction of species previously absent can lead to trophic shifts, attracting predators and restructuring the associated food web (Couce Montero et al., 2025; Reubens et al., 2014). Such changes can qualitatively alter ecosystem dynamics, emphasizing the need for long-term studies of artificial offshore structures.

#### 4.2. Biofouling growth patterns and quantification

Biofouling thickness and coverage are typically assessed in two ways: on test coupons that are designed to mimic real components in shape or material and during the early stages of research projects, or they can be directly assessed on actual structures after several years, often in the context of maintenance planning (e.g. 4–7 years in Picken, 1984; <4 years in Almeida and Coolen, 2020; >10 years in Boukinda Mbadinga et al., 2007). In terms of reference values, standards such as NORSOK (2007) provide benchmarks for established marine growth in the North Atlantic with a mean thickness of 100 mm observed between depths of 2 and 40 m, and 50 mm beyond 40 m. Decades ago, these types of values were already considered in the standard (Jusoh and Wolfram, 1996) on offshore oil platforms in the North Sea. This paper presents a complementary analysis in which these parameters are evaluated on an actual full-scale structure during the first years. The analyses carried out in this study revealed a significant relationship between biofouling thickness and coverage (Fig. 8). Although no statistically significant difference was found (Fig. 7A & B), a trend was observed indicating increased thickness near the surface and followed by a transition to lower thickness near the seabed. The thickness appears steady post-2021, with *Alcyonium digitatum* as the primary colonizer. Still, the average thickness

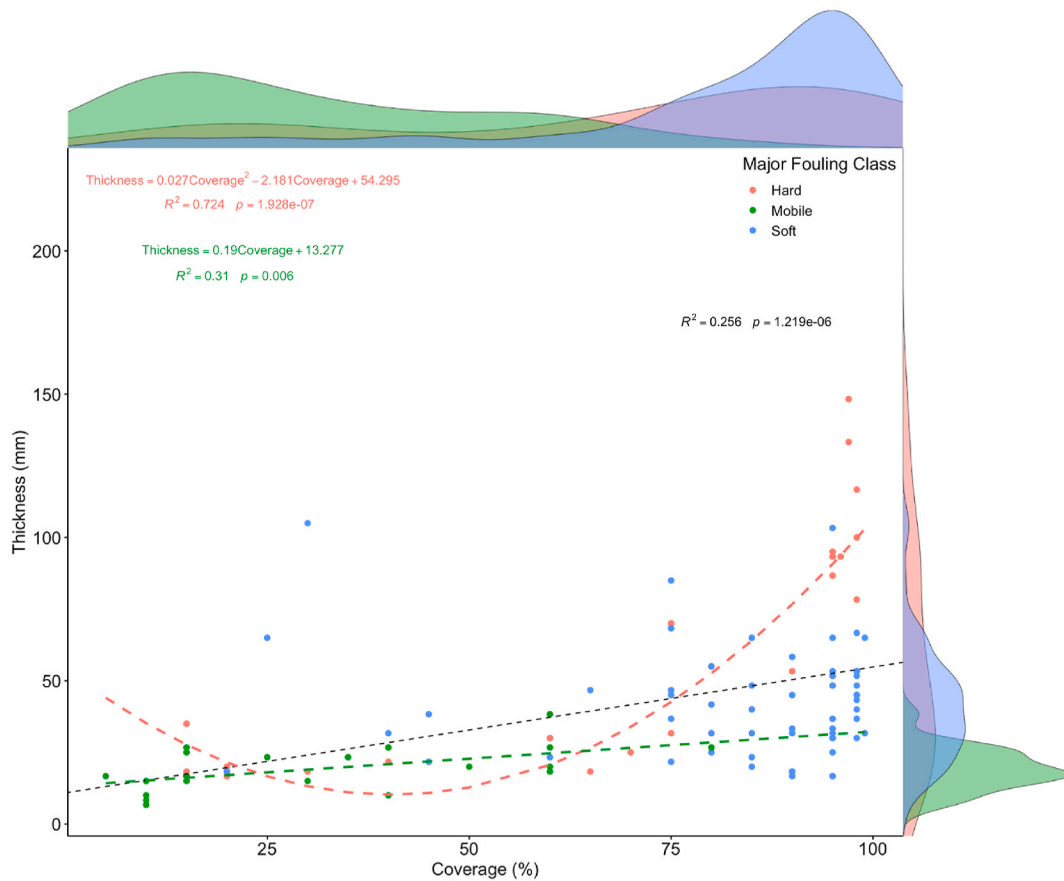


Fig. 8. Biofouling thickness in function of biofouling coverage depending on the major fouling class. Caption: on a sample (frame of analysis) the thickness and coverage were calculated and the main fouling class (most abundant) of the same sample was reported. Only significant models are shown in the figure.

should be approached with caution considering the average height of this species, which can readily attain 200 mm (Budd, 2008). Ultimately, statistics indicate the necessity of separating soft and hard fouling for the assessment of thickness and coverage percentage (Almeida and Coolen, 2020) as well as for conducting a targeted examination. This is further emphasized in the subsequent section, particularly when addressing issues of hydrodynamic engineering.

#### 4.3. Hydrodynamic implications of biofouling

The assessed and observed quantities of biofouling in this research are critical input data for the load computation of submarine cables:

- Qualitatively, the alteration in marine growth type modifies the shape exposed to the marine environment, thus affecting the hydrodynamic flow. Although the effects of various artificial shapes have been examined since the 1970s, beginning with Sarpkaya's (1976) pioneering research and subsequently by Wolfram and Naghipour (1999), the influence of actual shapes was studied more recently, particularly concerning hard fouling and, more specifically, mussels (Decurey et al., 2020; Warby et al., 2024). The roughness induced by biofouling has been shown to be the critical parameter for component fatigue. Nonetheless, the randomness of individual arrangements (Ameryoun et al., 2019; Schoefs et al., 2021) and the difficulty in evaluating this parameter under real conditions (O'Byrne et al., 2014) make a quantitative assessment of fine-scale roughness along the entire length of each line actually unattainable without meticulous sampling. Yet understanding the species involved elucidates the severity of colonization, as highlighted by

Signor et al. (2023), through a comparison of the impacts of barnacles, mussels and tubeworms.

- Quantitatively, the knowledge of biofouling thickness and type is essential for updating the weight, a key parameter for the static design and maintenance of mooring lines and dynamic power cables. It also helps in updating the conductivity, another crucial metric for the maintenance of dynamic power cables (Maksassi et al., 2022). Finally, the knowledge regarding the percentage of cover and thickness is essential for calculating dependability criteria (Schoefs and Tran, 2022), with the drag force being linearly dependent on the diameter (thickness) and the drag coefficient (percentage of cover and roughness). Schoefs et al. (2022) proposed an equation for computing the drag coefficient in steady flow:

$$C_{Ds} = M \left[ 1.3 - 0.76 \times e^{-14.5 \left( \frac{k/D}{D} \right)} \times e^{-0.23(SC)} \right] \quad (4)$$

Where  $M$  is a coefficient depending on the layers of biofouling,  $(k/D)$  represents the relative roughness and  $SC$  is the percentage of cover.

Understanding, measuring and monitoring these biological factors is critical, as their effects on maintenance have been demonstrated (Schoefs and Tran, 2022). Likewise, it has been shown (EMEC, 2018; Want et al., 2023) that omitting one cleaning visit per year can result in savings of up to 25,000 GBP. For a park of 10 offshore wind turbines over 25 years, this cost could represent almost 6 million GBP.

#### 5. Study limitations and recommendations for the industry

This study assessed biofouling communities over time on two mooring lines using ROV-collected data. While variations in ROV

models or operators led to inconsistencies in image quality across the survey period, the overall methodology still allowed the identification of trends and species. Consequently, the method remains a viable approach for the monitoring of submerged offshore structures and components. A standardized methodology is essential to improve data consistency and measurement reliability. Thus, recommended enhancements to ROV systems include the integration of a reference point (e.g. ruler, caliper, laser markers) for improved thickness measurement, as well as a robust diffusing lighting system and UHD-quality video acquisition. An additional significant update is the application of photogrammetry or stereoscopy, which could improve the reading and analysis of profiles along the line (O'Byrne et al., 2018a, 2018b). Automatic detection, classification and segmentation through machine learning are also promising methods (O'Byrne et al., 2018c, 2020). This facilitates cost-effective and time-efficient monitoring, provided it is executed properly (e.g. maintaining a constant low speed and measuring proximity to the substrate). It is strongly recommended to employ supplementary procedures, such as sample collection (e.g. quadrat scraping), to identify small and cryptic organisms residing within biofouling communities. This method, though necessitating increased financial and time investment and requiring an altered organizational framework, was efficient in the North Sea for Marine Renewable Energies infrastructures and NIS species, such as *Jassa marmorata* or *Monocorophium acherusicum*, which were detected using this approach (Coolen et al., 2018; De Mesel et al., 2015; Kerckhof et al., 2019; Mavraki et al., 2023). Such species might have gone unnoticed in this study under the NA data for instance. Moreover, another bias was possibly introduced in this study because only a visible surface was filmed ("apparent coverage"), which may be greater or equal to the real surface ("effective coverage") on the line. For example, the area covered by the pedial disk of *M. senile* on the mooring line should be the basis of the measurement. The direct measurement of this surface would compensate for this bias, as gaps may be present between each individual (Appendix 5). The implementation of a continuous monitoring program throughout the lifespan of the offshore structure is essential, as previously suggested and endorsed in multiple surveys (Almeida and Coolen, 2020; Boutin et al., 2023; Zupan et al., 2023). Unlike the method used in this study, multiple monitoring and sampling efforts should be executed to mitigate the impact of seasonal or exceptional events on the results and analysis. A study of lines subject to varying currents may reveal differences in the kinetics of colonization and community evolution.

## 6. Conclusion

This study examined biological colonization on two of the six mooring lines of France's inaugural floating offshore wind turbine FLOATGEN, using ROVs visual surveys. The analysis revealed a clear vertical distribution of biofouling communities: hard fouling, such as mussels, dominated the upper sections, while soft fouling taxa, including anemones and soft corals, became increasingly prevalent with depth. A dominance of soft fouling was observed over time in deeper sections of the mooring lines, resulting in notable increases in fouling coverage and thickness. In contrast, the upper sections showed greater inter-annual variability, including a peak in hard fouling thickness during one particular year. These trends translated into increases in mooring line thickness ranging from +7 % to +32 %, depending on the year and depth, which could have implications for structural loading over time.

The results underline the importance of robust and standardized monitoring protocols to accurately capture biofouling dynamics and their impacts on offshore infrastructure components. In particular, the use of high-resolution and calibrated recording significantly improves measurement precision and enables more reliable exploitation of visual data across varying coverage levels. Although the study does not directly assess structural or ecological impacts, it highlights the operational value of consistent visual monitoring for tracking long-term trends in fouling development. Future work could benefit from extending the

spatial range of observations or incorporating advanced imaging techniques to refine community analyses and support model calibration efforts. Another perspective relies on improving the quantification of the impact of marine growth on the reliability of synthetic mooring lines, especially concerning fatigue behavior (Pham et al., 2019b; Thuilliez et al., 2023).

## CRedit authorship contribution statement

**Antoine Dubois:** Writing – review & editing, Writing – original draft, Visualization, Formal analysis, Data curation, Conceptualization. **Franck Schoefs:** Writing – original draft, Funding acquisition, Formal analysis, Conceptualization. **Bruno Cognie:** Writing – review & editing, Resources, Conceptualization. **Marine Reynaud:** Writing – review & editing, Visualization, Resources. **Thomas Soulard:** Writing – review & editing, Validation, Resources. **Justine Dumay:** Writing – review & editing, Visualization.

## Declaration of competing interest

The authors declare the following financial interests/personal relationships which may be considered as potential competing interests: Schoefs Franck reports financial support was provided by WEAMEC Community. If there are other authors, they declare that they have no known competing financial interests or personal relationships that could have appeared to influence the work reported in this paper.

## Acknowledgments

This work is financially supported and part of the European Interreg Atlantic Area BlueGift project and by Centrale Nantes own funding. Biostatistical study were performed within the I2FLOW (Improve the Environmental Integration of Floating Offshore Wind Turbines) and MOORREEF within the Sea and Littoral Research Institute (IUML), Nantes Université, Nantes, France funded by European Community (FEDER) and WEAMEC community (cluster funded by Region Pays de la Loire). Authors are thankful to L. Barillé & V. Turpin for their relevant advice on statistics computing and to BW IDEOL for agreement on publication.

## Appendix A. Supplementary data

Supplementary data to this article can be found online at <https://doi.org/10.1016/j.ecss.2025.109302>.

## Data availability

Data will be made available on request.

## References

- Almeida, L.P., Coolen, J.W.P., 2020. Modelling thickness variations of macrofouling communities on offshore platforms in the Dutch North Sea. *J. Sea Res.* 156, 101836. <https://doi.org/10.1016/j.seares.2019.101836>.
- Ameryoun, H., Schoefs, F., Barillé, A.L., Thomas, Y., 2019. Stochastic modeling of forces on jacket-type offshore structures colonized by marine growth. *J. Mar. Sci. Eng. Sect. Ocean Eng. Mar. Struct.* 7 (5). <https://doi.org/10.3390/jmse7050158-2019>.
- Bishop, M.J., Mayer-Pinto, M., Airoidi, L., Firth, L.B., Morris, R.L., Loke, L.H.L., Hawkins, S.J., Naylor, L.A., Coleman, R.A., Chee, S.Y., Dafforn, K.A., 2017. Effects of ocean sprawl on ecological connectivity: impacts and solutions. *J. Exp. Mar. Biol. Ecol.* 492, 7–30.
- Boukinda Mbadanga, M.L., Schoefs, F., Quiniou, V., Birades, M., 2007. Marine growth colonisation process in Guinea gulf: data analysis. *J. Offshore Mech. Arctic Eng.* 129 (2), 97–106. <https://doi.org/10.1115/1.2355518>.
- Boutin, K., Gaudron, S.M., Denis, J., Ben Rais Lasram, F., 2023. Potential marine benthic colonisers of offshore wind farms in the English Channel: a functional trait-based approach. *Mar. Environ. Res.* 190, 106061. <https://doi.org/10.1016/j.marenvres.2023.106061>.

- Budd, G.C., 2008. 'Dead man's fingers (*Alcyonium digitatum*): marine evidence-based sensitivity assessment (MarESA) review'. <https://dx.doi.org/10.17031/marlinsp.1187.1>.
- Carrington, E., 2002. Seasonal variation in the attachment strength of blue mussels: causes and consequences. *Limnol. Oceanogr.* 47 (6), 1723–1733.
- Causon, P.D., Gill, A.B., 2018. Linking ecosystem services with epibenthic biodiversity change following installation of offshore wind farms. *Environ. Sci. Pol.* 89, 340–347. <https://doi.org/10.1016/j.envsci.2018.08.013>.
- Connor, D.W., Allen, J.H., Golding, N., Howell, K.L., Lieberknecht, L.M., Northen, K., Reker, J.B., 2004. *The Marine Habitat Classification for Britain And Ireland Version 04.05*. Peterborough. Joint Nature Conservation Committee.
- Coolen, J.W.P., Bos, O.G., Glorius, S., Lengkeek, W., Cuperus, J., Van der Weide, B.E., Agüera, A., 2015. Reefs, sand and reef-like sand: a comparison of the benthic biodiversity of habitats in the Dutch Borkum Reef Grounds. *J. Sea Res.* 103, 84–92.
- Coolen, J.W.P., van der Weide, B., Cuperus, J., Blomberg, M., Van Moorsel, G., Faasse, M. A., Bos, O.G., Degraer, S., Lindeboom, H.S., 2018. Benthic biodiversity on old platforms, young wind farms, and rocky reefs. *ICES (Int. Coun. Explor. Sea) J. Mar. Sci.* 77 (3), 1250–1265. <https://doi.org/10.1093/icesjms/fsy092>.
- Couce Montero, L., Abramic, A., Guerra Marrero, A., Espino Ruano, A., Jiménez Alvarado, D., Castro Hernandez, J., 2025. Addressing offshore wind farms compatibilities and conflicts with marine conservation through the application of modelled benchmarking scenarios. *Renew. Sustain. Energy Rev.* 207, 114894. <https://doi.org/10.1016/j.rser.2024.114894>.
- De Mesel, I., Kerckhof, F., Norro, A., Rumes, B., Degraer, S., 2015. Succession and seasonal dynamics of the epifauna community on offshore wind farm foundations and their role as stepping stones for non-indigenous species. *Hydrobiologia* 756, 37–50. <https://doi.org/10.1007/s10750-014-2157-1>.
- Decurey, B., Schoefs, F., Barillé, A.L., Soulard, T., 2020. Model of bio-colonisation on mooring lines: updating strategy based on a static qualifying sea state for floating wind turbines. *J. Mar. Sci. Eng. Sect. Ocean Eng. Spec. Iss. "Monit. Coast. Offshore Struct."* 8 (108). <https://doi.org/10.3390/jmse8020108>.
- Degraer, S., Brabant, R., Rumes, B., 2012. *Offshore wind farms in the Belgian part of the North Sea: Heading for an understanding of environmental impacts*. Brussels: royal Belgian Institute of natural sciences, OD natural environment. *Mar. Ecol. Manag.* 168.
- Degraer, S., Brabant, R., Rumes, B., Vigin, L., 2021. Environmental impacts of offshore wind farms in the Belgian part of the North Sea: attraction, avoidance and habitat use at various spatial scales. In: *Mar. Ecol. Manag. Memoirs on the Marine Environment*. Royal Belgian Institute of Natural Sciences, OD Natural Environment, Brussels, p. 104pp.
- Díaz, H., Guedes Soares, C., 2020. Review of the current status, technology and future trends of offshore wind farms. *Ocean. Eng.* 209, 107381. <https://doi.org/10.1016/j.oceaneng.2020.107381>.
- Elliott, M., Birchenough, S.N.R., 2022. Man-made marine structures – Agents of marine environmental change or just other bits of the hard stuff? *Marine Pollution Bulletin* 176, 113468. <https://doi.org/10.1016/j.marpolbul.2022.113468>.
- European Marine Energy Centre, EMEC, 2018. Press release: CleanWinTur biofouling solutions for offshore wind turbines. Available at: <https://www.emec.org.uk/press-release-cleanwintur-biofouling-solutions-for-offshore-wind-turbines/>.
- Hiscock, K., Wilson, E., 2007. 'Plumose anemone (*Metridium dianthus*): marine evidence-based sensitivity assessment (MarESA) review'. <https://dx.doi.org/10.17031/marlinsp.1185.2>.
- Jusoh, I., Wolfram, J., 1996. Effects of Marine Growth and Hydrodynamic Loading on Offshore Structures, vol. I. *Jurnal Mekanikal, Jilid*, pp. 77–98.
- Karlsson, R., Tivefålh, M., Duranović, I., Martinsson, S., Kjølhamar, A., Murvoll, K.M., 2022. Artificial hard-substrate colonisation in the offshore hywind Scotland pilot park. *Wind Energ. Sci.* 7, 801–814. <https://doi.org/10.5194/wes-7-801-2022>.
- Kerckhof, F., Degraer, S., Norro, A., Rumes, B., 2011. Offshore Intertidal Hard Substrata: a New Habitat Promoting Non-indigenous Species in the Southern North Sea: an Exploratory Study. Royal Belgian Institute of Natural Sciences.
- Kerckhof, F., Rumes, B., Degraer, S., 2019. About "mytilisation" and "slimeification": a decade of succession of the fouling assemblages on wind turbines off the Belgian coast. In: Degraer, S., Brabant, R., Rumes, B., Vigin, L. (Eds.), *Environmental Impacts of Offshore Wind Farms in the Belgian Part of the North Sea: Marking a Decade of Monitoring, Research and Innovation*. Brussels: Royal Belgian Institute of Natural Sciences, OD Natural Environment. *Marine Ecology and Management*, p. 134, 2019.
- Koehl, M.A.R., 1977. Effects of sea anemones on the flow forces they encounter. *J. Exp. Biol.* 69, 87–105.
- Leclerc, J.-C., Viard, F., Gonzalez-Sepulveda, E., Diaz, C., Neira Hinojosa, J., Pérez Aranedá, K., Silva, F., Brante, A., 2019. Habitat type drives the distribution of non-indigenous species in fouling communities regardless of associated maritime traffic. *Divers. Distrib.* 26, 62–75. <https://doi.org/10.1111/ddi.12997>.
- Lutrand, A., Houbin, C., Thiebaut, E., 2020. JD-1.1 Substrats artificiels du circalittoral du large. In: Rivière, La, et al. (Eds.), *Fiches descriptives des habitats marins benthiques de la Manche, de la Mer du Nord et de l'Atlantique*. *PatriNat (OFB-MNHN-CNRS)*, Paris, pp. 105–108, 2022.
- Maar, M., Bolding, K., Petersen, J.K., Hansen, J.L.S., Timmermann, K., 2009. Local effects of blue mussels around turbine foundations in an ecosystem model of Nysted offshore wind farm. *Den. J. Sea Res.* 62, 159–174. <https://doi.org/10.1016/j.seares.2009.01.008>.
- Maduka, M., Schoefs, F., Thiagarajan, K., Bates, A., 2023. Hydrodynamic effects of biofouling-induced surface roughness – review and research gaps for shallow water offshore wind energy structure. *Ocean. Eng.* 272. <https://doi.org/10.1016/j.oceaneng.2023.113798>–2023.
- Maksassi, Z., Garnier, B., Gueled, A., Schoefs, F., Schaeffer, E., 2022. Thermal characterization and thermal effect assessment of biofouling around a dynamic submarine electrical cable. *Energies* 15 (9). <https://doi.org/10.3390/en15093087>.
- Maksassi, Z., Ould, A., Garnier, B., Schoefs, F., Schaeffer, E., 2024. For better comprehension of mussel's thermal characteristics and their thermal effect on dynamic submarine electrical cables. *Appl. Ocean Res.* 144. <https://doi.org/10.1016/j.apor.2024.103900>.
- Mann, H.B., Whitney, D.R., 1947. On a test of whether one of two random variables is stochastically larger than the other. *Ann. Math. Stat.* 18 (1), 50–60.
- Markert, A., Esser, W., Frank, D., Wehrmann, A., Exo, K.-M., 2013. Habitat change by the formation of alien *Crasostrea*-reefs in the Wadden Sea and its role as feeding sites for waterbirds. *Estuar. Coast Shelf Sci.* 131, 41–51. <https://doi.org/10.1016/j.ecss.2013.08.003>.
- Marty, A., Berhault, C., Damblans, G., Facq, J.-V., Gaurier, B., Germain, G., Soulard, T., Schoefs, F., 2021. Experimental study of marine growth effect on the hydrodynamical behaviour of a submarine cable. *Appl. Ocean Res.* 114. <https://doi.org/10.1016/j.apor.2021.102810>.
- Marty, A., Schoefs, F., Damblans, G.C., Facq, J.-V., Gaurier, B., Germain, G., 2022. Experimental comparative study of two kinds of hard marine growth effects on the hydrodynamical behaviour of a cylinder submitted to wave and current solicitations. *Ocean. Eng.* 263. <https://doi.org/10.1016/j.oceaneng.2022.112194>.
- Mavraki, N., Bos, O.G., Vlaswinkel, B.M., Roos, P., de Groot, W., van der Weide, B., Bittner, O., Coolen, J.W.P., 2023. Fouling community composition on a pilot floating solar-energy installation in the coastal Dutch North Sea. *Front. Mar. Sci.* 10, 1223766.
- Miller, R.G., 1981. *Simultaneous Statistical Inference*. Springer.
- Nelson, M.L., Craig, S.F., 2011. Role of the sea anemone *Metridium senile* in structuring a developing subtidal fouling community. *Mar. Ecol. Prog. Ser.* 421, 139–149. <https://doi.org/10.3354/meps08838>.
- Niquil, N., Raoux, A., Haraldsson, M., Araignous, E., Halouani, G., Leroy, B., Safi, G., Nogués, Q., Grangeré, K., Dauvin, J.-C., Riera, F., Mazé, C., Le Loc'h, F., Villanueva, M.C., Hattab, T., Bourdaud, P., Champagnat, J., Ben Rais Lasram, F., 2020. Toward an ecosystem approach of marine renewable energy: the case of the offshore wind farm of courseulles-sur-mer in the bay of seine. In: Nguyen, K., Guillou, S., Gourbesville, P., Thiébot, K. (Eds.), *Estuaries and Coastal Zones in Times of Global Change*. Springer, Singapore. [https://doi.org/10.1007/978-981-15-2081-5\\_9](https://doi.org/10.1007/978-981-15-2081-5_9).
- NORSOK, 2007. *Actions and action effects*. N-003. Norway: standards Norway. Available at: <https://online.standard.no/en/norsok-n003-2007>.
- Oshurkov, V.V., 1992. Succession and climax in two fouling communities. *Biofouling: J. Bioadhesion Biofilm Res.* 6 (1), 1–12. <https://doi.org/10.1080/08927019209386205>.
- Osman, R.W., 1977. The establishment and development of a marine epifaunal community. *Ecol. Monogr.* 47, 37–63.
- O'Byrne, M., Ghosh, B., Pakrashi, V., Schoefs, F., 2014. *Effects of Turbidity and Lighting on the Performance of an Image Processing Based Damage Detection Technique*. Taylor & Francis, pp. 2645–2650.
- O'Byrne, M., Schoefs, F., Pakrashi, V., Ghosh, B., 2018a. A stereo-matching technique for recovering 3D information from underwater inspection imagery. *Comput. Aided Civ. Infrastruct. Eng.* 33 (3), 193–208. <https://doi.org/10.1111/mice.12307>.
- O'Byrne, M., Schoefs, F., Pakrashi, V., Ghosh, B., 2018b. An underwater lighting and turbidity image repository for analysing the performance of image based non-destructive techniques. *Struct. Infrastruct. Eng. Maint., Manag. Life-Cycle Des. Perform.* 14 (1), 104–123. <https://doi.org/10.1080/15732479.2017.1330890>.
- O'Byrne, M., Pakrashi, V., Schoefs, F., Ghosh, B., 2018c. Semantic segmentation of underwater imagery using deep networks. *J. Mar. Sci. Eng. Sect. Ocean Eng. Spec. Issue "Underw. Imaging 6 (3)"*. <https://doi.org/10.3390/jmse6030093>.
- O'Byrne, M., Pakrashi, V., Schoefs, F., Ghosh, B., 2020. Applications of virtual data in subsea inspections. *J. Marine Science and Engineering, section Ocean Engineering, Special Issue "Underwater Computer Vision and Image Processing 328 (5), 8"*. <https://doi.org/10.3390/jmse8050328>.
- PatriNat, 2023. *Table de correspondances entre la typologie nationale des habitats marins benthiques de la Manche, de la Mer du Nord et de l'Atlantique (NatHab-AtI) et la classification EUNIS 2022*.
- Pezy, J.-P., Raoux, A., Dauvin, J.-C., 2020. The environmental impact from an offshore windfarm: challenge and evaluation methodology based on an ecosystem approach. *Ecol. Indic.* 114, 106302. <https://doi.org/10.1016/j.ecolind.2020.106302>.
- Pham, H.-D., Schoefs, F., Soulard, T., Cartraud, P., Pham, H.H., Berhault, C., 2019a. Methodology for modelling and service life monitoring of mooring lines of floating wind turbines. *Ocean. Eng.* 193.
- Pham, H.-D., Cartraud, P., Schoefs, F., Soulard, T., Berhault, C., 2019b. Dynamic modeling of nylon mooring lines for a floating wind turbine. *Appl. Ocean Res.* 87, 1–8. <https://doi.org/10.1016/j.apor.2019.03.013>.
- Picken, G.B., 1984. The operational assessment of marine growth on offshore structures'. In: *5th Offshore Inspection Repair and Maintenance*, pp. 15–26. London: IRM/AODC Conference.
- Raoux, A., Dambacher, J.M., Pezy, J.-P., Mazé, C., Dauvin, J.-C., Niquil, N., 2018. Assessing cumulative socio-ecological impacts of offshore wind farm development in the Bay of Seine (English Channel). *Mar. Pol.* 89, 11–20. <https://doi.org/10.1016/j.marpol.2017.12.007>.
- Reubens, J.T., Degraer, S., Vincx, M., 2014. The ecology of benthopelagic fishes at offshore wind farms: a synthesis of 4 years of research. *Hydrobiologia* 727, 121–136. <https://doi.org/10.1007/s10750-013-1793-1>.
- Rife, G.S., 2018. Ecosystem services provided by benthic macroinvertebrate assemblages in marine coastal zones. *Ecosyst. Serv. Glob. Ecol.* 61–79.

- Sarà, M., 1986. Sessile macrofauna and marine ecosystem. *Ital. J. Zool.* 53 (4), 329–337. <https://doi.org/10.1080/11250008609355518>.
- Sarpkaya, T., 1976. In-line and transverse forces on smooth and sand-roughened cylinders in oscillatory flow at high Reynolds numbers. In: Monterey. Naval Postgraduate School, California.
- Schoefs, F., Tran, B., 2022. Reliability updating of offshore structures subjected to marine growth. *Energies*, section: B2: Wind, Wave and Tidal Energy, Special Issue: Reliability of Marine Energy Converters. Academic Editor: Dimitry Val, 15(2), 414. <https://doi.org/10.3390/en15020414>.
- Schoefs, F., Clément, A., Nouy, A., 2009. Assessment of ROC curves for inspection of random fields. *Struct. Saf.* 31 (5), 409–419. <https://doi.org/10.1016/j.strusafe.2009.01.004>.
- Schoefs, F., O'Byrne, M., Pakrashi, V., Gosh, B., Oumouni, M., Soulard, T., Reynaud, M., 2021. Fractal dimension as an effective feature for characterizing hard marine growth roughness from underwater image processing in controlled and uncontrolled image environments. *J. Mar. Sci. Eng.* 9 (12), 1344. <https://doi.org/10.3390/jmse9121344>.
- Schoefs, F., Bakhtiari, A., Ameryoun, H., 2022. Evaluating of hydrodynamic force coefficients in presence of biofouling on marine/offshore structures, a review and new approach. *Journal of Marine Science and Engineering*, J. Mar. Sci. Eng. sect. Ocean Eng.Fluid/Struct. interact. II/Fluid/Structure Interactions II 10 (5), 558. <https://doi.org/10.3390/jmse10050558>.
- Seed, R., Suchanek, T., 1992. Population and community ecology of *Mytilus*. *Dev. Aquacult. Fish. Sci.* 25, 87–169.
- Shi, W., Park, H.C., Baek, J.H., Kim, C.W., Kim, Y.C., Shin, H.K., 2012. Study on the marine growth effect on the dynamic response of offshore wind turbines. *Int. J. Precis. Eng. Manuf.* 13, 1167–1176. <https://doi.org/10.1007/s12541-012-0155-7>.
- Signor, J., Schoefs, F., Quillien, N., Damblans, G., 2023. Automatic classification of biofouling images from offshore renewable energy structures using deep learning. *Ocean Engineering* 288, 115928. <https://doi.org/10.1016/j.oceaneng.2023.115928>.
- Spielmann, V., Dannheim, J., Brey, T., Coolen, J.W.P., 2023. Decommissioning of offshore wind farms and its impact on benthic ecology. *J. Environ. Manag.* 347, 119022. <https://doi.org/10.1016/j.jenvman.2023.119022>.
- Thilleul, O., Perignon, Y., 2022. SEM-REV Metocean Design Basis, 1.3. <https://doi.org/10.5281/zenodo.6325718>.
- Thuilliez, H., Davies, P., Cartraud, P., Feuvrie, M., Soulard, T., 2023. Characterization and modelling of the dynamic stiffness of nylon mooring rope for floating wind turbines. *Ocean Eng.* 287, 115866. <https://doi.org/10.1016/j.oceaneng.2023.115866>.
- Torquato, F., Omerspahic, M.H., Range, P., Bach, S., Riera, R., Ben-Hamadou, R., 2021. Epibenthic communities from offshore platforms in the Arabian Gulf are structured by platform age and depth. *Mar. Pollut. Bull.* 173. <https://doi.org/10.1016/j.marpolbul.2021.112935>.
- Tyler-Walters, H., 2008. 'Common mussel (*Mytilus edulis*): marine evidence-based sensitivity assessment (MarESA) review'. <https://dx.doi.org/10.17031/marlinssp.1421.1>.
- van der Stap, T., Coolen, J.W.P., Lindeboom, H.J., 2016. Marine fouling assemblages on offshore gas platforms in the southern North Sea: effects of depth and distance from shore on biodiversity. *PLoS One* 11, e0146324.
- Vinagre, P.A., Simas, T., Cruz, E., Pinori, E., Svenson, J., 2020. Marine biofouling: a European database for the marine renewable energy sector. *J. Mar. Sci. Eng.* 8 (7), 495. <https://doi.org/10.3390/jmse8070495>.
- Want, A., Goubard, A., Jonveaux, S., Leaver, D., Bell, M.C., 2023. Key biofouling organisms in tidal habitats targeted by the offshore renewable energy sector in the North Atlantic include the massive barnacle *chirona hameri*. *J. Mar. Sci. Eng.* 11, 2168. <https://doi.org/10.3390/jmse11112168>.
- Warby, C., Dias, F., Schoefs, F., Pakrashi, V., 2024. An ecologically aware modification of the Morison equation for long term marine growth effects. *Mech. Res. Commun.* 139, 104293. <https://doi.org/10.1016/j.mechrescom.2024.104293>.
- Whomersley, P., Picken, G.B., 2003. Long-term dynamics of fouling communities found on offshore installations in the North Sea. *J. Mar. Biol. Assoc. U. K.* 83, 897–901.
- Wilcoxon, F., 1945. Individual comparisons by ranking methods. *Biometrics Bull.* 1 (6), 80–83.
- Wolfram, J., Naghipour, M., 1999. On the estimation of Morison force coefficients and their predictive accuracy for very rough circular cylinders. *Appl. Ocean Res.* 21 (6), 311–328. [https://doi.org/10.1016/S0141-1187\(99\)00018-8](https://doi.org/10.1016/S0141-1187(99)00018-8).
- Yandell, B.S., 1997. *Practical Data Analysis for Designed Experiments*. Chapman&Hall.
- Zeinoddini, M., Bakhtiari, A., Schoefs, F., Zandi, A.P., 2017. Towards an understanding of the marine fouling effects on VIV of circular cylinders: Partial coverage issue. *Biofouling* 33 (3), 268–280. <https://doi.org/10.1080/08927014.2017.1291803>.
- Zupan, M., Rumes, B., Vanaverbeke, J., Degraer, S., Kerckhof, F., 2023. Long-term succession on offshore wind farms and the role of species interactions. *Diversity* 15, 288. <https://doi.org/10.3390/d15020288>.